euronoise

Acoustical and optical measurements on a mixture of air microbubbles in water

Vincent Duro[a], Dominique Rajaona[a], Dominique Decultot[a] and Gerard Maze[b]

[a]LOMC FRE 3102 CNRS Groupes Ondes Acoustiques, Université du Havre (IUT), Place Robert Schuman, 76610 Le Havre, France
[b]LAUE, Université du Havre, Place Robert Schuman, F-76610 Le Havre, France
vincent.duro421@univ-lehavre.fr

An important challenge for current naval research is the modernization of battleships. Their target detection system must be increasingly efficient and they must be increasingly undetectable. Due to turbulent flows and bubbles, ship wakes are a detectable acoustic signature and ship bow waves disturb sonar detection. In this work, we study sound propagation through bubble clouds in water. We have developed an experimental set-up which permits us to acquire, in synchronization, acoustical signals and optical images. The phenomenon of bubble monopole resonance in very low frequency, related to bubble size, provokes effects of strong sound damping and sound speed dispersion. These experimental results, related to theoretical results, permit to estimated sizes and concentrations of bubbles. The acquired bubble images permit to know the real bubble sizes and concentrations, in order to correlate them with the experimental acoustical results. Air bubbles are generated with a high-pressure engine introduced into the host liquid medium. The generation process and the evolution of bubbles are detailed. We present in this work, theoretical results establishing a complex effective wave number characterizing the sound propagation in an effective medium.

1 Introduction

Bow waves disrupt sonar detection. The ship wake has long life duration and is a detectable acoustic sign from several hundred meters of the ship. These are elements of an important challenge for the current naval research in order to modernize its battleships. Consequently, to be efficient, modern battleships must be undetectable targets and must own the best means of target detection. This paper presents a step towards a final objective of acoustic characterization of a ship wake. Bubbles, which provoke the deterioration of ship propellers with cavitations phenomenon, are also the essential element making up the ship wake. In this work, we investigate experimental results on the interaction of an acoustic wave with a bubble cloud in water. Simultaneously and in correlation with these acoustical measurements, an optical device to acquire images of bubble clouds is realized. A description of the bubble generation method by a high-pressure engine and the evolution of bubbles after their injection into water is necessary to understand the experiment process. A characterization of experimental bubble clouds and a description of their time evolution are realized. In order to interpret these results, theoretical relations established by other authors, relating to bubble characteristics (radii, characteristic resonance frequencies and densities) and their effects of sound damping and sound velocity dispersion, are used.

2 Experimental set-up

2.1 Bubble generation mechanism

Several ways to create bubbles exist as air injection into water with an air pump. A water drop or jet falling on a plane water surface traps air in the form of bubbles. For instance, streams, pouring water, rivers, rain, and breaking waves create air bubbles [1]. With these methods of generation, bubbles of too large sizes are produced. Cavitation, electrolysis or encapsulated gas-filled micro-spheres are other sources of bubbles but our measurement conditions make them unpractical. In our experiment, micro-bubbles are created with a high-pressure engine and a water starting pistol. Figure 1 shows us the bubble generation mechanism and the time bubble evolution. Into high-pressure engine, water arrives from the grey nozzle (left) and goes out highly pressurized (here 70 bars) by the black nozzle (right) toward the water starting pistol. This last one permits a high speed flow of water which goes to trap air micro-bubbles into the pistol water.

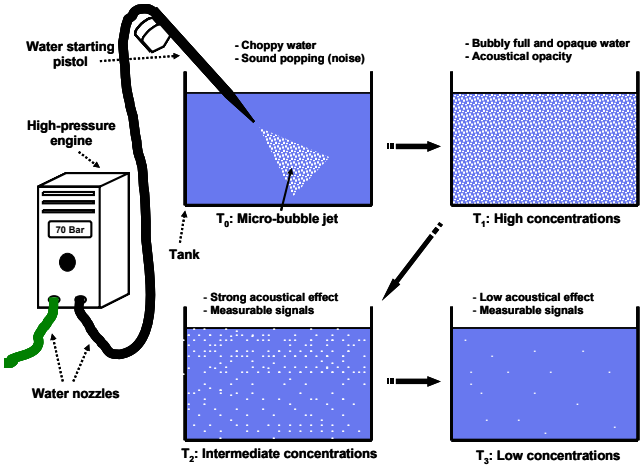

Fig.1 Sketch of bubble generation mechanism. Evolution of generated bubble cloud is decomposed in four steps.

The water jet impact on a plane water surface drives ambient air into water tank and generates other bubbles. To avoid that, the pistol output is introduced into water. During micro-bubble jet (Time T_0), the tank water is very choppy and a sound popping is produced by the bubble generation mechanism. The used transducers are saturated by generated noises which make erroneous measurements during the micro-bubble jet. During time T_1 , the tank water is bubbly full and becomes opaque optically and acoustically. After formation, bubbles rapidly accelerate to its terminal rising velocity determined by the balance between the buoyant rise force, and the drag force [2]. This velocity is a function of bubble size and is very slow for micro-bubbles. Motions in the fluid can affect this velocity. In our experiment, we observe first a transitional regime with motions in all directions which can last several minutes. Next, we observe a permanent regime where most micro-bubbles rise progressively toward the surface and collapse. Other micro-bubbles can collapse before to attain the surface. This second regime lasts much longer time than the first. Consequently, the bubble concentration diminishes progressively (Time T_2 and T_3) and acoustic measurements

become feasible. This experimental study is dependent of created bubble clouds which are not stationary, but the previous description is stayed globally legitimate at each experiment.

2.2 Measurement device

Figure 2 describes the layout of acoustical and optical sensors into and around the measurement tank, and elements of electronic device. We recall that the objective of this device is the simultaneous acquirement of bubble images and signals of acoustical waves propagating through the bubbly water. The bubbly water glass tank has 210 cm of length, 100 cm of width, 100 cm of height and 1 cm of wall thickness. It contains a water level of 90 cm. To transmit and to receive acoustical waves, two transducers (PANAMETRICS®) are used. Their central frequency is equal to 100 kHz with a frequency bandwidth usable between 30 and 170 kHz. The distance between them is equal to 130 cm. They are located at a depth of 50 cm, at 40 cm of the tank bottom and at 50 cm of the longest tank walls. A high power (500 mW to 1 W) laser generator (LASIRIS®) of wavelength between 670 nm and 810 nm is used to obtain a plane laser beam into water. The laser generator is fixed above the tank on a perpendicular axis at surface water. A distance of 65 cm separates this axis from transducers. The vertical plane laser beam is located at the tank centre and is contained in the transducers axis. Its thickness is equal to 0.2 cm at the transducers axis level. Generally used to flow visualization or 3D profiling, it is useful to improve the visualization of micro-bubbles making them fluorescent (white). At the tank outside, a video camera (JAI-PULNIX® TM-6740CL CCD 1/3") providing 200 images per second (fps) in full resolution of 640x480 pixels is used to detect images. A mono-focal high-resolution objective (TAMRON® 23FM50SP) having a focal distance of 50 mm is added to the camera and permits to obtain images focused only on the plane laser beam. Consequently, fluorescent micro-bubbles appear on images without magnification effects. The video camera is located at the same height that transducers and formed with the laser generator a perpendicular plan at the transducers axis. The distance between the camera objective and the longest tank wall is equal to 4 cm. In consequence, a distance of 55 cm separates the camera objective from the plane laser beam. In these conditions and using a ruler placed in the plane laser beam to calibrate the real image size, we have estimate one pixel to a value of 25 µm. The full image resolution becomes equal to 1.6x1.2 cm^2 (i.e. 1.92 cm^2). It is the best resolution that we have obtained with this equipment. Now, we detail the elements of electronic device. First, in the acoustical part, the emission is realized by a pulse generator (SOFRANEL PANAMETRICS® model 5052 UA) which emits a pulse signal toward a transducer at each external trigger. The transmitted acoustical wave is received by the other transducer, and the received signal is transmitted toward a signal amplifier (5 kHz – 1 MHz). The amplified signal is acquired by a numerical oscilloscope (LECROY® wave Runner 6051) at each external trigger. Second, the imaging part, the Camera Link Cable (KAB® Cameralink-A-10M) permits an instantaneous transfer of images toward the image acquisition input of the computer (IMASYS® speed video station) at each external trigger. The image trigger input is used to detect the trigger of acquisition frequency. The sequence trigger input is used to detect the start trigger of an acquisition sequence. These two inputs receive only TTL signals. The acquisition is realized by a digitization card (COIM® X64-CL IPRO), and another card I/O (Input/Output) is useful to the two inputs described previously. Additionally, to manage acquisitions, software (CVB® Image Manager-USB) is useful for image access and another (CVB HIRIS®-STREAMING) is useful for image sequence recording.

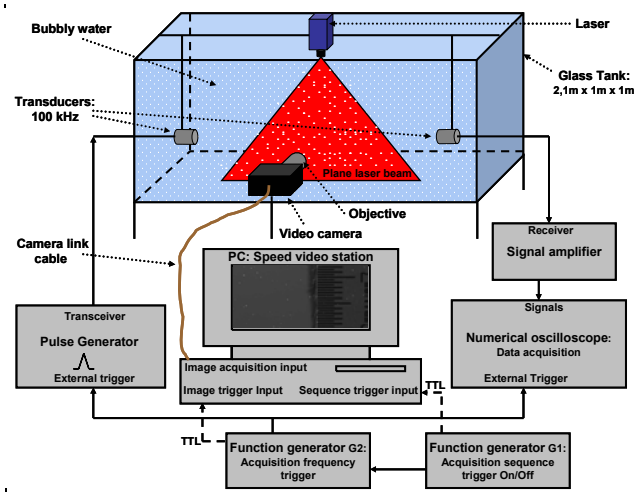

Fig.2 Sketch of measurement device for synchronized measurements of images and acoustical signals.

The control device is realized by two arbitrary function generators (SONY TEKTRONIX® AFG320) in order that we can decide on the acquisition sequence start. The acquisition frequency is equal to 2 Hz (i.e. a period $\Delta t = 0.5$ sec). The determination of the acquisition frequency lasts two pulses which introduces a delay of 1s between the start of image acquisition sequence and the start of signal acquisition sequence. During an experiment, 2400 acquisitions (i.e. 20 min) of images and signals are realized to study the micro-bubble cloud evolution. The recording starts just before the micro-bubble injection to have reference signals of sound propagation in the tank without micro-bubbles which is useful for a normalization of others signals. The image and signal treatment is realized later.

3 Theoretical study

3.1 The acoustic bubble

In this subsection, inspired by Überall works [3], we have determined the scattering function of a single spherical air bubble in water as

$$f_n(x) = \frac{2}{x}\sum_{n=0}^{\infty}(-1)^n(2n+1)\sqrt{A_n.A_n^*}\,, \qquad (1)$$

with x the dimensionless reduced frequency in water and A_n the backscattering amplitude. Figure 3 shows us resonance frequencies of an air bubble in water for vibration modes n = 0…11. We distinguish a high resonance peak (monopole resonance, n = 0) in very low

frequency (VLF) about x = 0.01391, and in high frequency (HF) the others resonances and overtones. In this paper, only the monopole resonance is studied. A relation between the monopole frequency f_0 and the equilibrium bubble radius R_0 have been deduced from Eq.(1) as

$$f_0 = \frac{0,01391.c_w}{2\pi R_0}, \qquad (2)$$

where c_w is the sound velocity in water. For example, a bubble radius equal to 30 µm resonates around 100 kHz. This zeroth mode is a simple volume pulsation with a radially symmetric in-and-out pulsating motion [4].

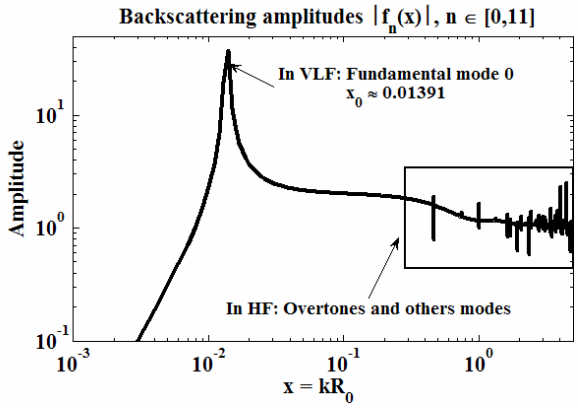

Fig.3 Backscattering amplitude modulus of an air bubble in water as a function of x for n = 0….11.

The transducers used in the experimental section have a frequency bandwidth between 30 to 170 kHz. This entrains that only bubbles having resonance frequencies into this frequency band could be detected by these transducers, i.e., bubbles having radii comprised between 20 and 100 µm.

3.2 Effective medium

Several approaches of effective medium theory have been developed to describe the linear wave propagation through a host liquid medium containing bubbles. However, we denote two pioneering approaches. First, the Foldy [5] approach which determines the total scattered field by the bubbly medium taking into account interactions of each bubble with the incident field and with the scattered fields by each of other bubbles. Specifying the mean pressure in the bubbly liquid, an effective wavenumber is found as

$$k_m^2 = k^2 + 4\pi N \Im, \qquad (3)$$

where $\Im$ is the scattering function of one bubble, N the bubble density and k the wavenumber. Medwin [6, 7] has investigated a second approach which consists of the expression of effective medium compressibility changes because of bubbles. The compressibility is made up of a part due to the bubble-free water and a part involving the change in volume of the bubbles. On these basis, Commander and Prosperetti [8] establishes an effective wavenumber which is given by

$$k_m^2 = \left(\frac{\omega}{c}\right)^2 + 4\pi\omega^2 \int_0^\infty \frac{R_0 n(R_0) dR_0}{\omega_0^2 - \omega^2 + 2ib\omega}, \qquad (4)$$

with ω_0 the bubble resonance frequency, ω the exciting frequency, $n(R_0)$ the bubble density and b a dissipative energy term. The velocity V_{Th} and the attenuation coefficient A_{Th} of sound in the bubbly water are found as

$$V_{Th} = \frac{\omega}{\mathrm{Re}\{k_m\}}, \qquad (5)$$

and

$$A_{Th} = 20(\log_{10} e)\,\mathrm{Im}\{k_m\}. \qquad (6)$$

In this paper, only the damping coefficient interests us. We have chosen an example of Gaussian bubble size distribution expressing as

$$n(R_0) = \begin{cases} n_0 \exp\left(\dfrac{-\left(R_0^{[n_0]} - R_0\right)^2}{2\sigma_0^2}\right) & if \quad R_0(\mu m) \in [25,35] \\ 0 \end{cases}, \qquad (7)$$

where $R_0^{[n_0]}$ is the central radius of the distribution for which the bubble density is maximal and is noted n_0. σ_0 is a parameter which has an influence on the Gaussian width.

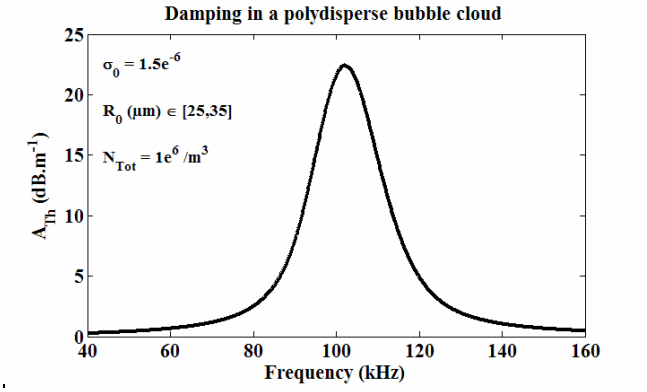

Fig.4 Damping (dB/m) versus frequency (kHz) produced by a polydisperse bubble cloud for a constant bubble number per unit volume equal to 10^6

The repartition in bubble size makes in order that the total bubble number N_{Tot} stays quasi-constant. The input parameters of the Gaussian function are $N_{Tot} = 10^6$, $\sigma_0 = 1.5e^{-6}$ and $R_0(\mu m) \in [25,35]$. From Eq.(2), we can determine that $f_0(kHz) \in [87,122]$. n_0 is equal to 130000 bubbles per unit volume, $R_0^{[n_0]}$ is equal to 30 µm and the corresponding resonant frequency $f_0^{[n_0]}$ is equal to 101 kHz. On figure 4, the black line curve represents the damping in dB/m, calculated with Eq.(6), as a function of the exciting frequency in kHz on an acoustical wave propagating through a bubble cloud in water. The bubble size distribution function of this cloud has been described previously. We observe a maximum damping in a frequency band near this of bubble resonance frequencies.

4 Experimental results

4.1 Acoustical part

In order that acoustic measurement may be legitimate, a necessary condition is the fact that the damped frequency band must be included into the frequency bandwidth of transducers.

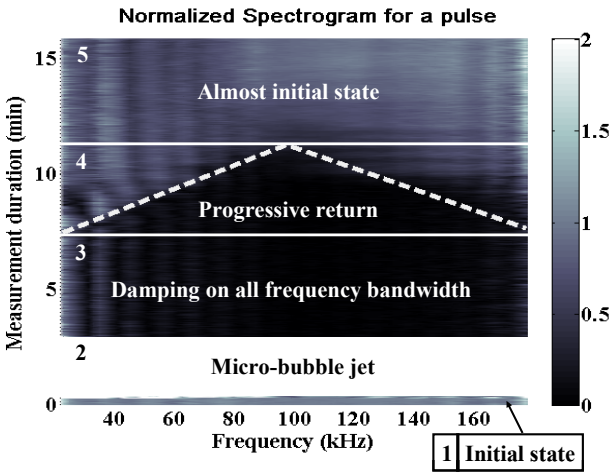

Fig.5 Normalized spectra evolution versus frequency during experiment of impulse responses of bubbly water

We note $S(f)$ the spectra of measured impulse responses in the bubbly water and $S_0(f)$ the initial spectrum without bubbles. $S(f)$ is normalized by $S_0(f)$ to correct frequency bandwidth of transducers and to avoid other outer effects not due to bubbles. Figure 5 shows the normalized spectra evolution versus frequency during experiment. Five steps are distinguished. First, the initial state (gray level = 1) without bubbles corresponds to $S_0(f)$ and lasts around 0.5 min. Secondly, during around 2 at 2.5 min, bubbles are introduced into water (white level). Just after bubble jet (Step 3) and during around 4.5 min, all frequency bandwidth is damped (black level). At the step 4, during around 3.5 min, spectra start to get back progressively their initial values but differently according to frequency. Dashed lines permit to remark that during this step the damping band narrows progressively. Additionally, the maximum of damping duration is around 100 kHz. Consequently, damping frequency bands include into transducer bandwidth and acoustic measurements become legitimate. Finally, step 5, spectra have come back an almost initial state (almost grey level). It is impossible to come back exactly the initial start state because a return at an equilibrium state of water lasts much time. Taking into account the distance D between transducers, the experimental damping A_{Exp} in dB/m is represented by the relation as

$$A_{Exp}(f) = \frac{20}{D}\log\left(\frac{S(f)}{S_0(f)}\right) \qquad (9)$$

For acoustical and optical measurements, to diminish errors, we have assumed that five successive measurements make very low changes. In consequence, one result at time t becomes the average of the measurement at this time t, the two previous times and the two following times.

4.2 Optical part

The elementary volume, observed by the camera, is equal to 1.6x1.2x0.2 cm^3. From the bubble number found in this volume, a bubble number is derived for a volume of 1 m^3. This small observation volume increases the error possibilities on bubble accounts. Nevertheless, when bubble number is sufficiently important, the results are significant because the probability of bubble presence on images is sufficiently important. On the contrary, if bubble number is too low, this probability becomes also too low and we obtain hazardous results even with an average of five consecutive measurements. Using imaging software, images are made binary in white and black with a threshold optimizing bubble detection. The bubble accounts are realised by object form recognition. Then, the object surface is calculated and we assign at each object (i.e. each bubble) an equivalent radius corresponding to a circle radius having the same surface.

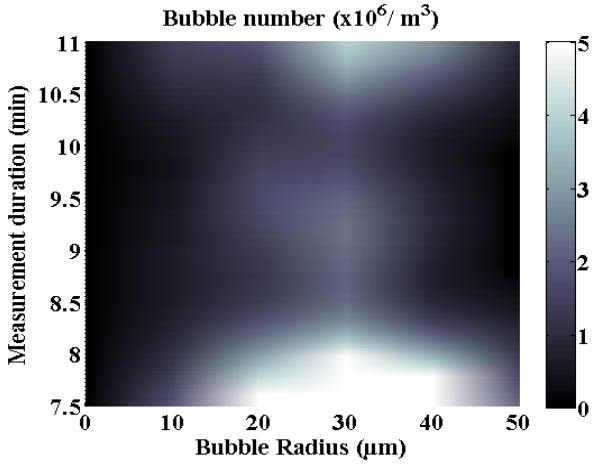

Fig.6 Bubble number evolution per m^3 of water versus bubble radii during experiment

Figure 6 shows us bubble number evolution per m^3 of water versus bubble radius during experiment from 7.5 to 11 min. It corresponds to step 4 described in the previous subsection. We observe that bubble sizes are centered around 30 µm and are comprised at the maximum between 10 and 50 µm. Bubble numbers don't exceed 10^7. Before 7.5 min (step 3), bubbles and bubble sizes are more numerous. That explains why all transducer bandwidth is damped in acoustical part. From around 11 min, we observe that bubble numbers increase but we think these values are erroneous because from this time of measurement the probability of bubble presence on images was very low. This hypothesis is verified in the acoustical part since from this time acoustical damping effects are almost finished.

5 Discussion and conclusion

We assume that the experimental bubble clouds have a Gaussian bubble size distribution function. To determine this distribution function, we use a statistical approach researching the values of Gaussian function parameters which minimize the Mean Quadratic Error (EQM) between

the experimental damping A_{Exp} and a theoretical estimated damping A_{Th}^{*} as

$$\min\left[\frac{1}{N_{\omega}}\sum_{1}^{N_{\omega}}\left(A_{Th}^{*}-A_{Exp}\right)^{2}\right], \qquad (8)$$

with N_{ω}, the element number into A_{Exp} where each element corresponds to each measurement frequency.

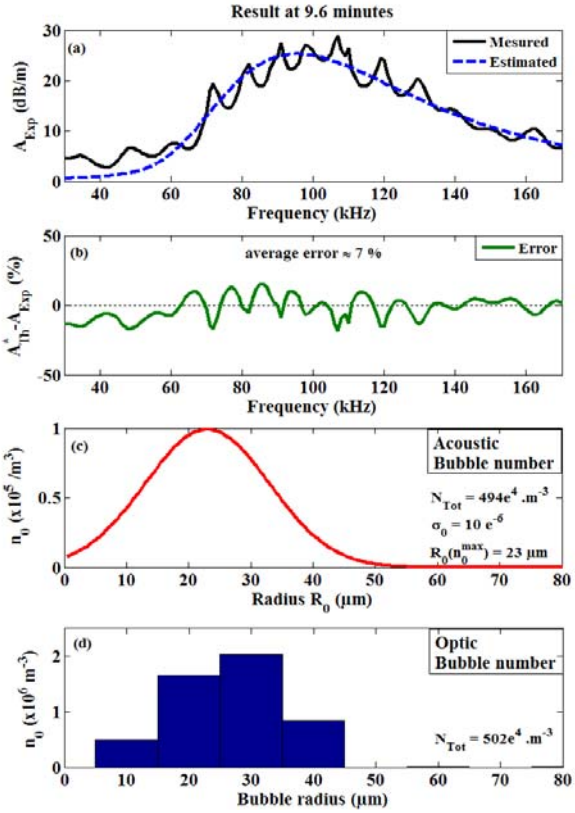

Fig.7 Result at time 9.6 minutes.
(a) Measured (Line) and estimated damping (Dash). (b) Error between them. (c) Bubble number via acoustical method. (d) Bubble number via optical method.

Figure 7 shows us an example of result obtained at time 9.6 min. On curves 7a, we observe both measured (Solid line) and estimated (dashed line) damping in the acoustical part. Curve 7b represents relative errors between them. With an average error of 7 %, we can say that there is a good agreement between them. Curve 7c is the Gaussian distribution giving the estimated damping. Curve 7d is the distribution obtained by optical method. We remark the measured bubble sizes and the total bubble number are almost equivalent. On the contrary, the bubble number by size is different but that is due to a different size sampling between acoustical and optical methods. The following Table 1 gives the time evolution of total bubble number obtained by both methods between times 8.1 and 10 min which is the period where measurement conditions were optimal in the two cases.

	Evolution of total bubble number N_{Tot} (x10^6 /m^3)									
Time (min)	**8.1**	**8.3**	**8.5**	**8.8**	**9**	**9.2**	**9.4**	**9.6**	**9.8**	**10**
Acoustic	**8**	**7.5**	**5**	**5**	**5**	**5**	**5**	**4.94**	**4.88**	**2.53**
Optic	**11.24**	**7.6**	**5.56**	**4.97**	**5.07**	**5.43**	**5.42**	**5.02**	**4.59**	**4.45**
Error	**3.2**	**0.1**	**0.56**	**0.03**	**0.07**	**0.43**	**0.42**	**0.08**	**0.29**	**1.92**

Table 1 Comparison between evolutions of total bubble number obtained by acoustical and optical methods

It shows us again a good agreement between results of these two methods. In conclusion, the bubble size distribution can be estimated by acoustical damping measurements even if it is difficult to find optimal measurement conditions. Additionally, we have assumed the bubble cloud had a Gaussian size distribution function. We may improve these results using random bubble size distribution functions. Another acoustical method to estimate bubble size distribution is the sound phase speed measurement in relation to Eq.(5) [9].

Acknowledgments

The authors are grateful to Bassin d'Essais des Carènes (France) and to the Région Haute-Normandie (France) for their financial support.

References

[1] Kees van den Doel "Physically-based models for liquid sounds", *Proceedings of ICAD 04-Tenth Meeting of the International Conference on Auditory Display, Sydney, Australia,* July 6-9, 2004

[2] "Bubble hydrodynamics", *Bubbleology.com*

[3] K. A. Sage, J. Georges and H. Überall "Multipole resonances in sound scattering from gas bubbles in a liquid", *J. Acoust. Soc. Am.* 65(6), 1413-1413 (1979)

[4] T. G. Leighton "The acoustic bubble", Chap.3 129-286 1994

[5] E. L. Carstensen and L. L. Foldy "Propagation of sound through a liquid containing bubble", *J. Acoust. Soc. Am.* 19, 481-501 (1947)

[6] H. Medwin and C. Clay "Fundamentals of acoustical oceanography", Chap.8 287-347 1998

[7] H. Medwin "Acoustic fluctuations due to microbubbles in the near-surface ocean", *J. Acoust. Soc. Am.* 56, 1000-1004 (1974)

[8] K. W. Commander, A. Prosperetti "Linear pressure waves in bubbly liquids: Comparison between theory and experiments", *J. Acoust. Soc. Am.* 85(2), 732-746 (1989)

[9] V. Duro, D. Décultot, G.Maze "Multiple scattering of acoustical waves in a bubbly liquid medium: Comparison between theoretical and experimental results", *Proceedings of the institute of Acoustics Meeting of the International Conference on Detection and Classification of Underwater Targets, Edinburgh, Scotland,* 97-104 , September 18-19, 2007